J Mol Model (2013) 19:1967–1972
DOI 10.1007/s00894-012-1548-3

ORIGINAL PAPER

Computational study of Be_2 using Piris natural orbital functionals

Jon M. Matxain · Fernando Ruipérez · Mario Piris

Received: 27 April 2012 / Accepted: 23 July 2012 / Published online: 1 September 2012

Abstract The third (PNOF3), fourth (PNOF4) and fifth (PNOF5) versions of the Piris natural orbital functional were used to characterize the beryllium dimer. The results obtained were compared to those gained afforded by CASSCF and CASPT2 as well as experimental data. The equilibrium distances (R_e), dissociation energies (D_e), effective bond orders (EBOs), and rovibrational levels were calculated. PNOF3, PNOF4, and CASPT2 predicted a bonded Be_2 molecule, while PNOF5 and CASSCF did not, which demonstrates the importance of the dynamical electron correlation. We observed that PNOF3 yields the most accurate equilibrium distances, while PNOF4 most accurately calculates the rovibrational levels. However, both of these functionals overestimate dissociation energies. Both PNOF3 and PNOF4 predict EBOs that agree with that obtained using CASPT2.

Keywords Natural orbital functional theory · PNOF · Dynamical correlation · Beryllium dimer

Introduction

The Be dimer is, a priori, one of the simplest molecules encountered in chemistry. It is composed of two beryllium atoms with "only" eight electrons. From both theoretical and experimental perspectives, it would therefore be easy to assume that the characterization of this molecule (in terms of its equilibrium distance and other properties) would be relatively easy. However, this is not the case. The Be_2 molecule has long been a challenge to experimentalists and theoretical chemists.

In the late 1920s and early 1930s, the whole chemistry community believed that the beryllium dimer was unstable. Based on early theoretical calculations and experimental observations, it was thought that beryllium gas remained monoatomic [1–6]. Much later, in the 1970s and 1980s, theoretical and experimental evidence for bonding in Be_2 was found [7–9]. Based on high-level theoretical calculations [7, 8], a relatively short equilibrium distance of around 2.5 Å was accepted, even though some authors claimed that Be_2 was characterized by van der Waals bonding with an equilibrium distance of around 5 Å. This fact was confirmed in 1984, when, for the first time, the Be_2 molecule was measured experimentally, and the first experimental spectrum of Be_2 was obtained [10–12]. The equilibrium geometry was found to be 2.45 Å, with an approximate dissociation energy (D_e) of 790±30 cm^{-1}. This experimental confirmation motivated a number of theoretical and experimental investigations aimed at accurately determining the dissociation energy. Recently, Merritt et. al. [13] accurately measured the dissociation energy as 929.7±2.0 cm^{-1}, confirming the theoretical prediction of Patkowski et. al. [14], who calculated a D_e of 938± 15 cm^{-1} based on a high level of theory.

The recent experimental work by Merritt et. al. [13] provided accurate experimental information on all of the bound vibrational levels of the ground state of Be_2, along with the potential energy curve, which

J. M. Matxain (✉) · F. Ruipérez · M. Piris
Faculty of Chemistry, University of the Basque Country (UPV/EHU), and Donostia International Physics Center (DIPC), P.K. 1072,
20080 Donostia, Euskadi, Spain
e-mail: jonmattin.matxain@ehu.es

M. Piris
IKERBASQUE, Basque Foundation for Science,
48011 Bilbao, Euskadi, Spain

significantly differs from other curves of related closed-shell metal atom dimers like Mg_2, Ca_2, Zn_2 and Hg_2. In these cases, a typical Morse-like curve is obtained, while the shape is quite different for Be_2. For theoreticians, these results can be taken as benchmark data for the development of novel theoretical methods. Indeed, as the authors mentioned in the conclusions of their paper [13], "Our experimentally determined potential energy curve establishes a benchmark for tests of high-level theoretical methods for treatment of configurational mixing and electron correlation." One of these novel methods is the natural orbital functional (NOF) theory.

The NOF theory [15–19] has emerged in recent years as an alternative method to conventional ab initio approaches and density functional theory (DFT) for considering electronic correlation. A major advantage of the NOF method is that the kinetic energy and the exchange energy are explicitly defined using the one-particle reduced density matrix (1-RDM) and do not require the construction of a functional. The unknown functional only needs to incorporate electron correlation. Further details and valuable literature on NOF theory can be found in [20, 21].

One route [22, 23] to the construction of an approximate NOF involves the use of a reconstruction functional based on the cumulant expansion [24–26] of the two-particle reduced density matrix (2-RDM). We shall use the reconstruction functional proposed in [27], in which the two-particle cumulant is explicitly reconstructed in terms of two matrices, $\Delta(\mathbf{n})$ and $\Pi(\mathbf{n})$, where $\mathbf{n}$ is the set of occupation numbers. The $\Delta(\mathbf{n})$ and $\Pi(\mathbf{n})$ matrices satisfy the well-known necessary N-representability conditions [28] and sum rules for the 2-RDM or, equivalently, the functional. Moreover, precise constraints that the two-particle cumulant matrix must fulfill in order to conserve the expectation values of the total spin and its projection have been formulated and implemented for the matrices $\Delta(\mathbf{n})$ and $\Pi(\mathbf{n})$ [29]. Appropriate forms of the matrices $\Delta(\mathbf{n})$ and $\Pi(\mathbf{n})$ lead to different implementations of the NOF, known in the literature as PNOFi (i=1–5) [27, 30–33]. This work is concerned with the last three implementations.

In PNOF3, we consider the opposite-spin components of the two-electron cumulant, but the Hartree–Fock (HF) approximation is used to account for most of the correlation effects between electrons with parallel spins. PNOF3 performs outstandingly well for atoms and molecules [31]. Moreover, this functional even accurately describes the topology of challenging potential energy surfaces [34]. Unfortunately, closer analysis of the dissociation curves for various diatomics [32], as well as the descriptions of diradicals and diradicaloids [35], revealed that PNOF3 overestimates the amount of electron correlation when orbital near-degeneracy effects become important. We demonstrated that this inaccuracy is related to the violation of the N-representability conditions, particularly the **G**-positivity condition [32]. Accordingly, PNOF3 is a suitable NOF for systems where static correlation effects are not important.

In order to rigorously comply with the N-representability conditions (the **D**-, **Q**-, and **G**-positivity conditions) of the 2-RDM, we developed a more restricted functional, PNOF4 [32]. Since the variational domain is more constrained, the percentage of the correlation energy recovered is less in PNOF4 than in PNOF3. However, it has been shown that PNOF4 is qualitatively better than its predecessor due to its capacity to accurately describe molecules with electrons that occupy orbitals which become increasingly degenerate [32, 35, 36]. Unfortunately, variational approaches under the necessary **D**-, **Q**-, and **G**-positivity conditions can lead to incorrect dissociation limits, with fractional numbers of electrons on the dissociated atoms [37, 38]. We have found fractional numbers of electrons to occur in several homolytic molecular dissociations when PNOF4 is used.

In order to remedy these problems, we simplified our approximations for $\Delta(\mathbf{n})$ and $\Pi(\mathbf{n})$ in the formulation of PNOF5. We assumed a HF-like product for the 2-RDM if $q \neq p,\tilde{p}$, which means that all off-diagonal terms are neglected except one, $\Delta_{p\tilde{p}}$ and $\Pi_{p\tilde{p}}$, respectively. There is no constraint that fixes the actual p and $\tilde{p}$ orbitals that are paired during the orbital optimization process, so the orbital pairing scheme varies during the optimization process until the most favorable orbital interactions are found. Obviously, similar to PNOF4, PNOF5 recovers lower correlation energies than PNOF3. However, a performance assessment has shown that PNOF5 correctly describes the equilibrium regions and the dissociation limits of diatomic molecules, yielding integer numbers of electrons on the dissociated atoms [33, 39]. This functional is able to describe diradicals and diradicaloids as well [40]. The oustanding agreement of the PNOF5 occupancies with those obtained by the CASSCF method represents an improvement over the PNOF4 results for these systems [35]. Consequently, PNOF5 yields remarkably accurate descriptions of systems with substantial (near-)degeneracy of one-particle states.

Methods

The aim of the work described in the present paper was to test the performance of PNOF3, PNOF4, and PNOF5 in describing the Be dimer. It is well known that this system presents mostly dynamical correlation effects, so we expected to achieve better descriptions using PNOF3 and PNOF4 than PNOF5. For comparison, CASSCF

[41–43] and CASPT2 [44, 45] calculations were also carried out, using an active space of four electrons in eight orbitals (4,8). All of these methods were combined with the cc-pVTZ basis set [46]. We calculated potential energy curves, equilibrium distances (R_e), dissociation energies (D_e), effective bond orders (EBOs, calculated as half of the difference between the occupation numbers of the bonding and antibonding orbitals) at equilibrium, and rovibrational levels, which were also compared to the experimental data available in [13]. We hoped that this work would provide us with fundamental new insights into the nature of electron correlation in this challenging molecule, as well as the performances of the different PNOFs.

Results and discussion

Figure 1 depicts the calculated HF, CASSCF, CASPT2, PNOF3, PNOF4, and PNOF5 relative potential energy curves for Be_2. Note that, for each curve, infinite distance corresponds to zero energy. Therefore, all of the curves were calculated relative to their own dissociation limits. The calculated R_e, D_e, and EBO values are collected in Table 1.

Let us first focus on the shapes of the calculated curves. Note that the HF method does not predict bonding in the Be_2 molecule. The electronic structure of Be_2 is $1\sigma_g^2\left(1\sigma_u^*\right)^2 2\sigma_g^2\left(2\sigma_u^*\right)^2$, so its EBO is 0. CASSCF is known to consider mainly nondynamical electron correlation effects, and these effects must be accounted for to correctly describe a Be atom. However, considering only nondynamical electron correlation is not sufficient to predict a minimum in the Be_2 potential energy curve, although CASSCF predicts an EBO of 0.2 at 2.38 Å (the R_e for CASPT2). The inclusion of dynamical correlation (via CASPT2) clearly improves the result. CASPT2 predicts an equilibrium distance of 2.38 Å with a dissociation energy of 789 cm^{-1}. The predicted equilibrium geometry is too short, and dissociation energies are somewhat low compared to the experimental data. This can be attributed to the size of the basis set, which is critical for CASSCF/CASPT2 calculations.

Table 1 R_e (Å), D_e (cm^{-1}), and EBO values calculated with the HF, CASSCF, CASPT2, PNOF3, PNOF4, and PNOF5 methods

	R_e	D_e	EBO
HF	–	–	0
CASSCF	–	–	0.20
CASPT2	2.38	789.0	0.20
PNOF5	2.23	−1187.8	0.40
PNOF4	2.61	2114.0	0.16
PNOF3	2.46	2518.9	0.20
Experimental	2.45	929.7	–

The PNOF5 functional is known to recover most of the nondynamical correlation and part of the dynamical correlation [33, 39]. Consequently, PNOF5 results occur midway between the CASSCF and CASPT2 results. It does predict a minimum that is shorter than CASPT2 one, at 2.23 Å, but this minimum is calculated to be metastable; that is, the dissociation energy is negative (−1187.8 cm^{-1}). However, the barrier is sufficiently large (1536.5 cm^{-1}) to allow for stable vibrational levels, as will be shown later. However, an unphysical cusp appears at around 2.6 Å. This cusp appears because the attractive ground state (corresponding to two interacting Be atoms) crosses a repulsive excited state (corresponding to two noninteracting Be atoms), as depicted in Fig. 2. The dissociative curve associated with noninteracting atoms should always be less stable

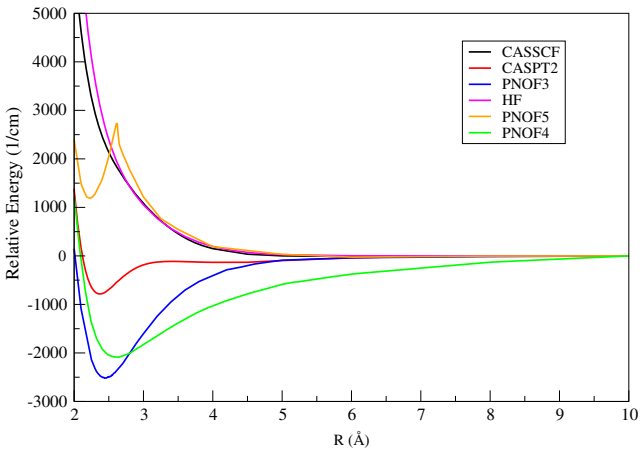

Fig. 1 Potential energy curves obtained with the HF, CASSCF, CASPT2, PNOF3, PNOF4, and PNOF5 methods

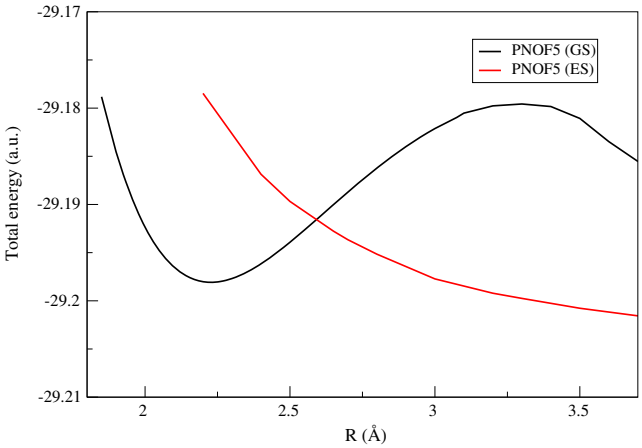

Fig. 2 Crossing of the ground-state (*GS*) and excited-state (*ES*) curves for Be_2 when PNOF5 is used

Table 2 Vibrational levels (cm^{-1}) and rotational constants B_v (cm^{-1}) calculated using CASPT2, PNOF3, PNOF4, and PNOF5, as well as corresponding experimental data taken from [13]

	CASPT2		PNOF3		PNOF4		PNOF5		Experimental	
v	E_{rel}	B_v	E_{rel}	B_v	E_{rel}	B_v	E_{rel}	B_v	E_{rel}	B_v
0	0.00	0.646	0.00	0.614	0.00	0.540	0.00	0.747	0.00	0.609
1	270.7	0.595	302.4	0.591	205.7	0.509	477.0	0.733	222.6	0.562
2	462.7	0.508	580.9	0.571	369.9	0.470	953.2	0.714	397.1	0.509
3	505.6	0.223	842.4	0.545	533.3	0.452	–	–	518.1	0.424
4	532.5	0.253	1074.8	0.521	672.8	0.427	–	–	594.8	0.355

than the attractive one. We think that the crossing predicted by PNOF5 is a consequence of its inability to account for some of the dynamical correlation. Therefore, one should beware of using PNOF5 when dynamical electron correlation effects are dominant, especially in weakly interacting systems like Be_2 or van der Waals complexes.

The PNOF3 and PNOF4 functionals recover the dynamical correlation and so are able to predict a stable Be_2 molecule. PNOF3 predicts a R_e value of 2.46 Å, very close to the experimental value of 2.45 Å. However, it clearly overestimates the dissociation energy. This is due to the fact that PNOF3 does not fullfil the required **G**-positivity condition of the two-particle reduced density matrix (2-RDM) [32]. When this violation is very small, PNOF3 is known to be very accurate [34, 47]. In the case of Be_2, the maximum violation of the **G** condition at equilibrium is −0.089, while the maximum violation at the dissociation limit is −0.019. The consequence of this is that the calculated total energy is accurately calculated at the dissociation limit but overestimated at equilibrium, so the calculated dissociation energy is overestimated. On the other hand, the calculated EBO is very similar to that calculated at the CASSCF/CASPT2 level of theory.

PNOF4 does not predict the equilibrium distance as accurately as PNOF3 does, but it does yield a more accurate dissociation energy. Note that PNOF4 satisfies the known necessary **D**-, **Q**-, and **G**-positivity (*N*-representability) conditions of 2-RDM, and does not overestimate total energies. However, the dissociation energy is still overestimated, due to a poorer description of the Be atoms at the dissociation limit. The calculated EBO is 0.16, somewhat smaller than that calculated at the CASSCF/CASPT2 and PNOF3 levels of theory.

In addition to equilibrium distances and dissociation energies, the shape of the potential energy curve is also very important, since it determines the rovibrational levels of the system. From Fig. 1, it is clear that the shapes of these curves differ significantly. In order to compare them with experimental data, we calculated the rovibrational levels from the CASPT2, PNOF3, PNOF4, and PNOF5 curves, and the values obtained are given in Table 2. The lowest five vibrational levels, along with their coupled rotational constants (B_v), were

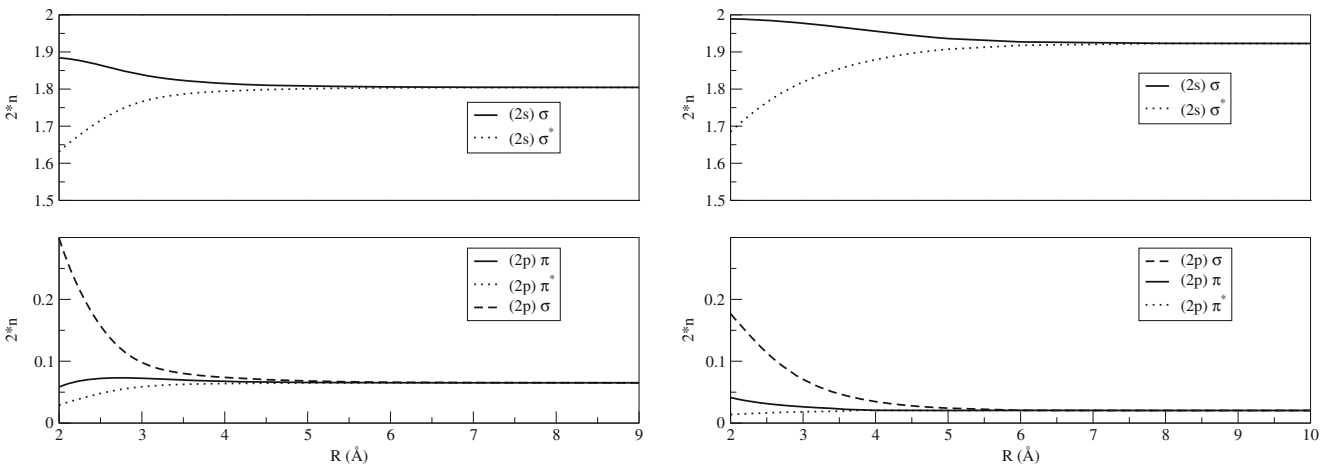

Fig. 3 Occupation numbers as a function of Be–Be distance. *Left*: CASSCF; *right*: PNOF3

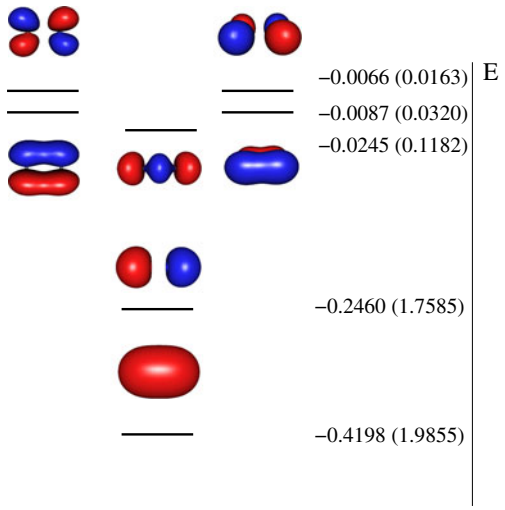

Fig. 4 Electronic configuration of Be_2 in the equilibrium region, calculated at the PNOF3/cc-pVTZ level of theory. The corresponding diagonal Lagrange multiplier (in hartrees) and occupation number (shown in parentheses) is given for each orbital

calculated. Comparing the data in Table 2, it is apparent that PNOF4 provides the closely agreement with the experimental data [13]. Notice that the PNOF4 curve is wide and highly anharmonic, as is the experimental curve (see Fig. 3 of [13]). The CASPT2 values are in quite good agreement with the experimental data, but the obtained values show that the curve is less anharmonic than for PNOF4 and the experimental curve near the equilibrium region. The PNOF3 curve is narrower and not very anharmonic, so the calculated levels are more widely separated. The agreement with the experimental results is worse than for PNOF4 and CASPT2. This can be adscribed to overestimation of the energy in the minimum region, which implies that the potential well is deeper and therefore narrower. Finally, PNOF5 is able to predict three stable vibrational levels. However, note that the curve is very narrow, which implies that the vibrational levels are much higher than in the experimental data.

Finally, in Fig. 3 the occupation numbers of PNOF3 and CASSCF are depicted as a function of the bond distance. The PNOF3 orbitals obtained at the minimum, along with their corresponding Lagrange multipliers and occupation numbers, are given in Fig. 4. Observe that, in the equilibrium region, there is charge transfer—mainly from the antibonding $2\sigma_u^*$ (2*s*) orbital to the bonding $3\sigma_g$ (2*p*) and $3\pi_u$ (2*p*) orbitals. As a consequence (as mentioned above), the EBO is around 0.2. This small EBO is in agreement with the observed weak Be–Be interaction. Note that, at the dissociation limit, the occupancies belong to two equivalent Be atoms, which is the correct behavior. From Fig. 3, it is clear that both the $2\sigma_g$ (2*s*) and $2\sigma_u^*$ (2*s*) orbitals converge to similarly occupied 2*s* atomic orbitals. In the same way, the molecular $3\sigma_g$ (2*p*), $3\sigma_u^*$ (2*p*), $3\pi_u$ (2*p*), and $3\pi_g^*$ (2*p*) orbitals dissociate to six equivalent *p* orbitals (three per atom).

Conclusions

In summary, in this work, we have demonstrated the performances of different PNOFs in the calculation of Be_2. We have shown the importance of including dynamical electron correlation in calculations aimed at predicting a stable dimer. Methods that do not include dynamical electron correlation, such as HF or CASSCF, predict dissociative curves, while PNOF5—which includes part of the dynamical correlation—predicts a metastable dimer. PNOF3 and PNOF4, like CASPT2, predict a stable dimer. PNOF3 predicts a very accurate equilibrium bond distance, 2.46 Å, which is only 0.01 Å larger than the experimental value. CASPT2 predicts a distance that is too short, while that afforded by PNOF4 is too large. Regarding dissociation energies, CASPT2 slightly underestimates the energy compared to the experimental value, while PNOF4 and—especially—PNOF3 overestimate it. Finally, PNOF4 predicts rovibrational levels more accurately than the other methods. The main drawback of PNOF5 is the fact that it does not account for part of the dynamical correlation. Including the remaining dynamical correlation in PNOF5 would, in principle, improve its performance.

Acknowledgments Financial support comes from Eusko Jaurlaritza (GIC 07/85 IT-330-07 and S-PC11UN003) and the Spanish Office for Scientific Research (CTQ2011-27374). The SGI/IZO–SGIker UPV/EHU is gratefully acknowledged for generous allocation of computational resources. JMM would like to thank the Spanish Ministry of Science and Innovation for funding through a Ramon y Cajal fellowship position (RYC 2008-03216).

References

1. Herzberg G (1929) Z Phys 57:601
2. Herzberg L (1933) Z Phys 84:571
3. Fraga S, Ransil BJ (1961) J Chem Phys 35:669
4. Fraga S, Ransil BJ (1962) J Chem Phys 36:1127
5. Bender CF, Davidson ER (1967) J Chem Phys 47:4972
6. Bartlett JH Jr, Furry WH (1931) Phys Rev 38:1615
7. Lengsfield BH III, McLean AD, Yoshimine M, Liu B (1891) J Chem Phys 1983:79
8. Harrison RJ, Handy NC (1983) Chem Phys Lett 98:97
9. Brom JM Jr, Hewett WD Jr, Weltner W Jr (1975) J Chem Phys 62:3122
10. Bondybey VE, English JH (1984) J Chem Phys 80:568
11. Bondybey VE (1984) Chem Phys Lett 109:436
12. Bondybey VE (1985) Science 227:125
13. Merritt JM, Bondybey VE, Heaven MC (2009) Science 324:1548
14. Patkowski K, Podeszwa R, Szalewics K (2007) J Phys Chem A 111:12822
15. Gilbert TL (1975) Phys Rev B 12:2111
16. Levy M (1979) Proc Natl Acad Sci USA 76:6062

17. Valone SM (1980) J Chem Phys 73:1344
18. Levy M (1987) Density matrices and density functionals. In: Erdahl R, Smith VH Jr (eds) Density matrices and density functionals. Reidel, Dordrecht, p 479
19. Cioslowski J (2005) J Chem Phys 123:164106
20. Piris M (2007) Natural orbital functional theory (chapter 14). In: Mazziotti DA (ed) Reduced-density-matrix mechanics: with applications to many-electron atoms and molecules. Wiley, Hoboken, p 387
21. Piris M (2012) Int J Quantum Chem. doi:10.1002/qua.24020
22. Piris M, Otto P (2003) Int J Quantum Chem 94:317
23. Piris M, Otto P (2005) Int J Quantum Chem 102:90
24. Valdemoro C (1992) Phys Rev 45:4462
25. Mazziotti DA (1998) Chem Phys Lett 289:419
26. Kutzelnigg W, Mukherjee D (1999) J Chem Phys 110:2800
27. Piris M (2006) Int J Quantum Chem 106:1093
28. Mazziotti DA (2012) Chem Rev 112:244
29. Piris M, Matxain JM, Lopez X, Ugalde JM (2009) J Chem Phys 131:021102
30. Piris M, Lopez X, Ugalde JM (2007) J Chem Phys 126:214103
31. Piris M, Matxain JM, Lopez X, Ugalde JM (2010) J Chem Phys 132:031103
32. Piris M, Matxain JM, Lopez X, Ugalde JM (2010) J Chem Phys 133:111101
33. Piris M, Lopez X, Ruipérez F, Matxain JM, Ugalde JM (2011) J Chem Phys 134:164102
34. Lopez X, Piris M, Matxain JM, Ugalde JM (2010) Phys Chem Chem Phys 12:12931
35. Lopez X, Ruipérez F, Piris M, Matxain JM, Ugalde JM (2011) ChemPhysChem 12:1061
36. Lopez X, Piris M, Matxain JM, Ruipérez F, Ugalde JM (2011) ChemPhysChem 12:1673
37. van Aggelen H, Bultinck P, Verstichel B, van Neck D, Ayers PW (2009) Phys Chem Chem Phys 11:5558
38. van Aggelen H, Verstichel B, Bultinck P, van Neck D, Ayers PW, Cooper DL (2010) J Chem Phys 132:114112
39. Matxain JM, Piris M, Ruipérez F, Lopez X, Ugalde JM (2011) Phys Chem Chem Phys 13:20129
40. Lopez X, Ruipérez F, Piris M, Matxain JM, Matito E, Ugalde JM (2012) J Comp Theor Chem. doi:10.1021/ct300414t
41. Roos BO, Taylor PR, Siegbahn PEM (1980) Chem Phys 48:157
42. Siegbahn P, Heiberg A, Roos BO, Levy B (1980) Phys Script 21:323
43. Siegbahn PEM, Heiberg A, Almlof J, Roos BO (1981) J Chem Phys 274:2384
44. Andersson K, Malmqvist P, Roos BO (1992) J Chem Phys 96:1218
45. Andersson K, Malmqvist P, Roos BO, Sadlej AJ, Wolinskit K (1990) J Phys Chem 94:5483
46. Dunning TH (1989) J Chem Phys 90:1007
47. Matxain JM, Piris M, Lopez X, Ugalde JM (2010) Chem Phys Lett 499:164